# Nanostructure Origins of $C_{60}$ Fluorescence in Pyridine

**Fang Zhang and Yan Fang***

*Beijing Key Lab for Nano-photonics and Nano-structure, Department of Physics, Capital Normal University, Beijing 100037, People's Republic of China*

*Received: November 29, 2005; In Final Form: March 21, 2006*

The nanostructure origins of three distinct and strong fluorescence bands of $C_{60}$ in room-temperature pyridine are reported for the first time. Fluorescence study and in-situ TEM observation on $C_{60}$-pyridine solutions with different setting times exhibit that the blue fluorescence peaks centered at 440 nm originate from $C_{60}$ nanoparticles; the yellow-green fluorescence band located at 575 nm derives from $C_{60}$ lace-like cluster; and the salmon pink fluorescence band around 700 nm arises from $C_{60}$ microbulk in solution. The conclusions are supported further by investigation on the $C_{60}$-toluene system as well.

## Introduction

Since photoluminescence of $C_{60}$ has a potential application in areas such as optics, electrics, materials science, and biomedicine,[1−3] investigating the emission mechanism to achieve high-quality fluorescence of $C_{60}$ is of great significance. However, due to low fluorescence quantum yield, induced not only by the intersystem crossing from singular state to the excited triplet state but also by the forbidden electronic transitions resulted from the high symmetry of $I_h$,[4−6] it is difficult to observe fluorescence from isolate $C_{60}$. Although well-resolved fluorescence spectra from $C_{60}$ in solids and glassy organic solvents have been reported due to the low-temperature-induced symmetry reduction,[7−12] to the best of our knowledge, room-temperature fluorescence spectra of $C_{60}$, obtained both in common solvents and on various substrates, are either incomplete or less resolved to date.[13,14]

In contrast, in the range from 425 to 764 nm, our recent successful observation of a series of strong fluorescence peaks from room-temperature $C_{60}$-pyridine solution discloses a potential application of $C_{60}$ as a novel white light photosensitive and luminescent material.[15] Nonetheless, even though consensus on solvent-induced reduction[16] of the $I_h$ symmetry and thus increase of fluorescence radiation rate seems to exist, theoretical or experimental evidence acquired so far are still not persuasive enough for revealing the origin of the rich and distinct fluorescence of $C_{60}$ in pyridine. According to linear solvation energy (LSER)[17] analysis on the solubility of $C_{60}$, three solid phases of $C_{60}$ might exist in the supersaturate solution, including solvate, solvate crystalline, and unsolvated $C_{60}$. Hence, in accordance with the X-traps scheme[18] interpreting that electronic state of $C_{60}$ may change with the particular environment, we presume that different emission centers might exist to be responsible for the fluorescence bands from $C_{60}$-pyridine solution.

In this paper, fluorescence measurements and simultaneous transmission electron micrograph (TEM) observations on supersaturated $C_{60}$-pyridine solutions were carried out in an effort to elucidate the generation of $C_{60}$ fluorescence in pyridine at room temperature. Three nanostructure origins, including $C_{60}$ nanoparticles, $C_{60}$ lace-like cluster, and $C_{60}$ micron bulk, are reported for the three strong fluorescence emission bands of $C_{60}$ in room-temperature pyridine first. The conclusions are further supported by investigations on the $C_{60}$-toluene system as well.

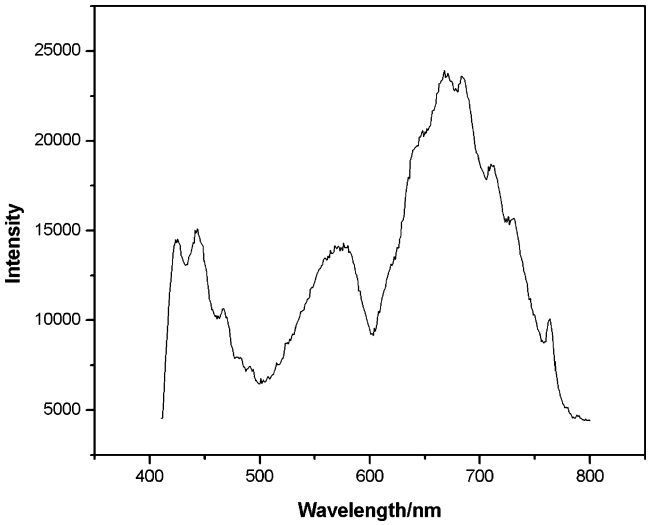


**Figure 1.** Fluorescence spectrum of $C_{60}$ in pyridine at room temperature, excited at 400 nm.

## Experimental Section

A total of 10 mg of $C_{60}$ (99.9%) was ultrasonically dissolved in 10 mL of pyridine (HPLC grade) for 10 h to form a brown supersaturated solution, and 3.0 mg/mL $C_{60}$-toluene solution was prepared through the same method. The fluorescence spectra were recorded by Fluorolog-3 spectrometer (JY), excited at 400 nm, with the excitation and emission slit widths being 5 nm. $C_{60}$ solutions with different setting time were doped on the surface of ultrathin carbon film and dried at room temperature before being taken as TEM samples. The TEM images were obtained by H600TEM (HiTachi), and the magnification is in the range from $5 \times 10^3$ to $1 \times 10^5$. The centrifugation of the $C_{60}$-pyridine solution was performed at 1200 revolutions/s for 5 min by employing a TDL-50B centrifugal separator. All the measurements were taken at room temperature.

## Results and Discussion

The fluorescence spectrum of 1.3 mg/mL $C_{60}$ in pyridine is exhibited in Figure 1. As we can see, three strong fluorescence bands (centered at 440, 575, and 700 nm, respectively) are obtained. Particularly, the blue fluorescence band is composed of five sharp peaks at 425, 443, 465, 480, and 490 nm. The yellow-green fluorescence band seems to include two peaks at

10.1021/jp056922b CCC: $33.50 
Published on Web 04/15/2006

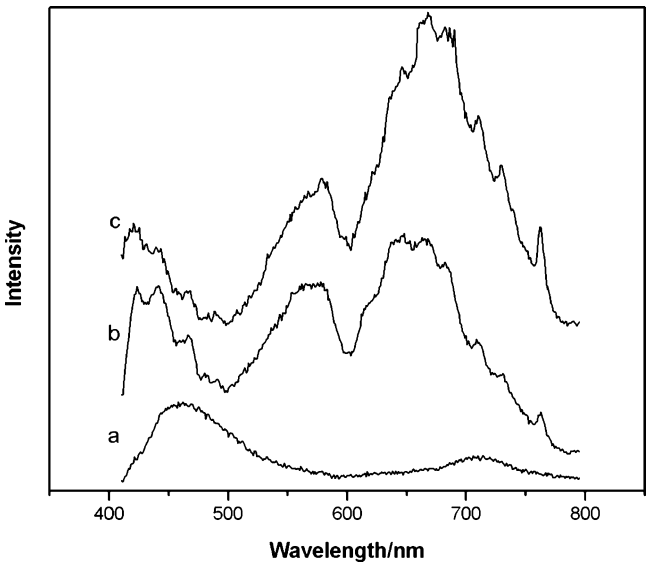


**Figure 2.** Fluorescence spectra of $C_{60}$-pyridine solutions settled for (a) 7 days, (b) 7 h, and (c) 7 min.

557 and 575 nm. The wide salmon pink fluorescence band also slips into seven peaks at 616, 646, 668, 685, 712, 730, and 764 nm. Owning to such rich fluorescence emission, the $C_{60}$-pyridine system, being superior to the yellow-green luminescent LED[19] that stirred wide interest among researchers, has a significant potential of being novel $C_{60}$-based white light photosensitive and luminescent material.

To investigate the mechanism of $C_{60}$ luminescence emission in pyridine, the fluorescence measurements and TEM observations were taken on $C_{60}$-pyridine solutions. First of all, fluorescence spectra were obtained at 7 min, 7 h, and 7days after the ultrasonication preparation process of the $C_{60}$-pyridine solution in sequence. Figure 2a displays the fluorescence spectrum of 1.0 mg/mL $C_{60}$-pyridine solution settled for 7 days. As we can see, in addition to a broad emission band centered at 700 nm, a blue band centered at 440 nm is present with approximately two times stronger intensity. Simultaneously, the general existence of isolated $C_{60}$ nanoparticles in this solution can be exhibited by a TEM image (Figure 3a). It noticed not only that the maximum diameter of the $C_{60}$ nanoparticles is about 250 nm but also that each $C_{60}$ nanoparticle consists of a number of smaller $C_{60}$ grains with diameters about several nanometers (Figure 3b). This provides a visible evidence for the analysis on $C_{60}$ solubility by Kaneto et al.[20] that the $C_{60}$ molecule in solution is not singly isolated but forms a finite cluster assembled with several $C_{60}$ molecules. Anyway, it can be clarified that $C_{60}$ molecules dissolved in solution are in the existence of nanoparticles.

What is the reason for $C_{60}$ nanoparticles existing as stable in pyridine? With the fact in mind that $C_{60}$ is an energetic electron acceptor and pyridine is an electron donor, we conjecture that interaction with little charge-transfer could occur between them, and thus an electropositive solvent cage of pyridine for $C_{60}$ nanoparticles would be formed. Therefore, due to the repulsion between solvent cages, $C_{60}$ nanoparticles are not easy to assemble with each other in solution.

Furthermore, because of the large specific surface area of the $C_{60}$ nanograin mentioned above, most of the $C_{60}$ molecules are located at the interface between $C_{60}$ and solvent (i.e., the $C_{60}$ molecule in nanoparticle has adequate opportunities to interact strongly with pyridine). As a result, solvent-induced symmetry degradation of $C_{60}$ would generate $C_{60}$ nanoparticle as a fluorescence emission center. As far as the main fluorescence emission of this solution is concerned (Figure 2a), it is not difficult to draw a conclusion that the blue fluorescence band centered at 440 nm probably originates from $C_{60}$ nanoparticles in solution, as is also supported by a reflection of the vibronic sidebands of $C_{60}$ from the fine structure of this blue

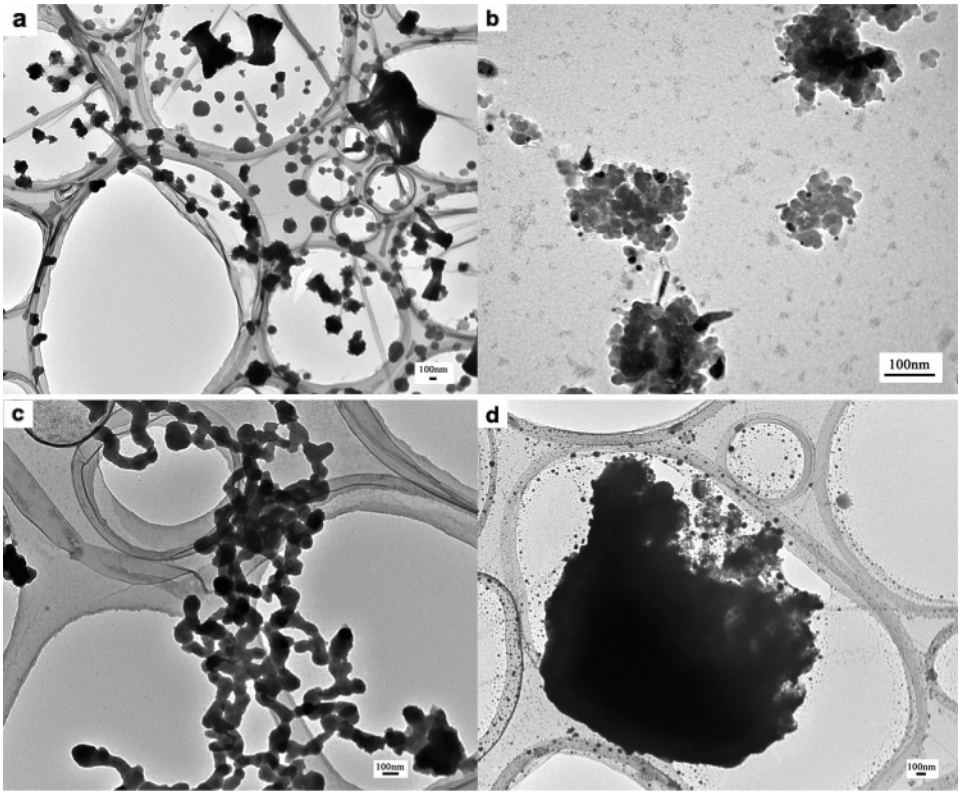


**Figure 3.** TEM images of $C_{60}$-pyridine solutions settled for (a) 7 days, (b) 7 days, (c) 7 h, and (d) 7 min.

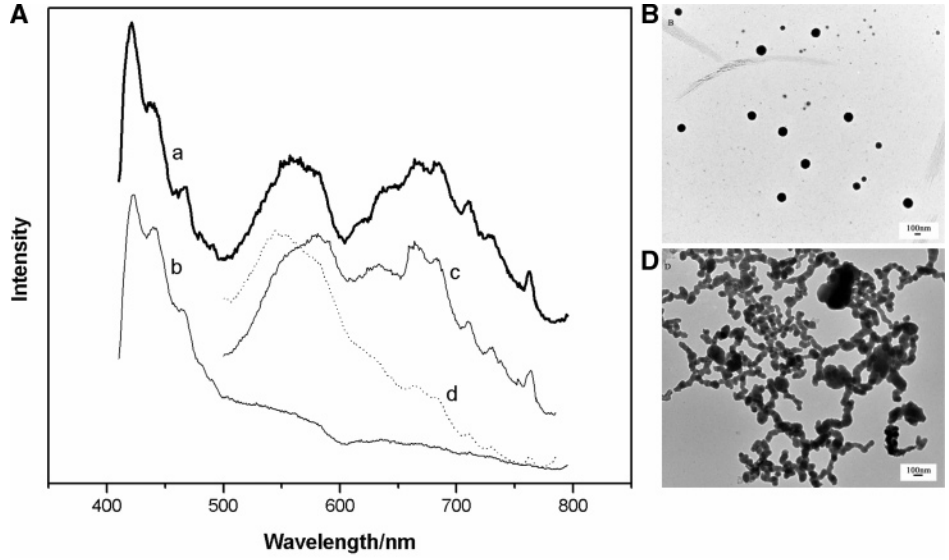


**Figure 4.** (A) Fluorescence spectra of (a) $C_{60}$-pyridine solution; (b) the up layer $C_{60}$-pyridine solution after centrifugation; (c) the low layer $C_{60}$-pyridine solution after centrifugation; and (d) the low layer $C_{60}$-pyridine solution after several processes of dilution and centrifugation. In-situ TEM images corresponding to (B) spectrum b and (D) spectrum d.

fluorescence band shown in Figure 1, in view of the energy intervals between adjacent peaks corresponding well with the surface-enhanced Raman spectrum of $C_{60}$ in pyridine at 772 $cm^{-1}$ [0.09 ev, $H_g(4)$], 574 $cm^{-1}$ [0.11 ev, $T_{1u}(2)$], 710 $cm^{-1}$ [0.14 ev, $H_g(3)$], 772 $cm^{-1}$ [0.09 ev, $H_g(4)$], and 496 $cm^{-1}$ [0.06 ev, $A_g(1)$], respectively.[21]

In addition to $C_{60}$ nanoparticles, there are also a few micron $C_{60}$ solid blocks in the range from 600 to 1320 nm (Figure 3a), which indicates the existence of "unsolvated $C_{60}$" in supersaturated solution. The weak fluorescence band located at 700 nm (Figure 2a), matching very well the 20 K luminescence spectrum of solid $C_{60}$ film deposited on $CaF_2$[22] and especially the luminescence spectrum of polycrystalline solid at 5 K,[12] is presumed to arise from these micron blocks of $C_{60}$ in solution, as is to be discussed in detail later.

To interpret the generation of fluorescence bands centered at 575 and 700 nm, fluorescence measurements and TEM observations were carried out on 1.0 mg/mL $C_{60}$-pyridine solution after setting the sample for 7 h. As is exhibited, three strong fluorescence bands are emitted from this solution (Figure 2b) in the company with a large number of $C_{60}$ lace-like clusters (Figure 3c) coming into sight in addition to the identical $C_{60}$ nanoparticles and micron $C_{60}$ blocks observed previously. Noticeably, the spherical $C_{60}$ nanoparticles in the clusters have similar diameters as the ones that are isolated in the solution.

How is the cluster formed in the solution? Why was it not observed in the solution that was settled for longer time? It is proposed that the characteristic interaction between $C_{60}$ and pyridine plays a crucial role in the formation of the $C_{60}$ lace-like cluster. In the beginning of the supersonic dissolution process, as is shown previously, $C_{60}$ is distributed into the solution in the existence of isolated nanoparticles wrapped in the solvent cage of pyridine. However, with the concentration increasing, a clash between $C_{60}$ nanoparticles would in turn be intense enough to break the solvent cage of isolated $C_{60}$ nanoparticle and stimulate the formation of a mutual solvent cage around several $C_{60}$ nanoparticles. This signifies the combination of $C_{60}$ nanoparticles (i.e., the formation of $C_{60}$ lace-like clusters). Additionally, the intertwining of lace-like clusters may directly result in the final deposition of $C_{60}$ clusters with large accumulated mass when the supersaturate $C_{60}$-pyridine solution was settled for a long enough time. Compared with the $C_{60}$ molecules in nanoparticles, $C_{60}$ in cluster might become a unique fluorescence emission center due to the extra restriction effect from the lace-like chain. Furthermore, taking the case in Figure 2a as a reference, the emergence of a novel yellow-green fluorescence band with the presence of $C_{60}$ lace-like clusters in solution definitely explicates that the fluorescence band centered at 575 nm may derive from the $C_{60}$ lace-like cluster.

Moreover, Figure 3b also displays a stronger and more informative fluorescence band around 700 nm than the counterpart shown in Figure 3a. As we can see, the separate lines in the salmon pink fluorescence are in good agreement with the fluorescence lines obtained from crystalline $C_{60}$ at 1.2K.[7] Especially, the fluorescence peak at 730 nm corresponds well with the line that is interpreted as fluorescence from $C_{60}$ molecules located in a perfect crystal environment.[18] Thus, unsolvated bulk $C_{60}$ in supersaturated solution would be estimated to be responsible for the fluorescence emission centered at 700 nm. To establish this assumption tentatively, a different fluorescence spectrum was obtained by reducing the settle time to 7 min (Figure 2c). Taking Figure 2b as a reference, there is a dramatic increase in the relative intensity of the salmon pink fluorescence band with more unslovated micron $C_{60}$ blocks present as shown in Figure 3d.

As is well-reported, the interaction of $C_{60}$ molecules in room-temperature solid film is not so strong as to induce structured fluorescence emission.[20] While, a weak electron−electron repulsion in a delocalized system (viz., the solvent-induced distortion of molecule in the solid matrix) would create $C_{60}$ in micron blocks as a somewhat well-resolved fluorescence emission center.[23] Thus, according to the further enhancement in relative intensity of fluorescence around 700 nm together with the increasing amount of micron $C_{60}$ blocks in solution, the fluorescence emission centered at 700 nm would be ascribed to $C_{60}$ microblocks in the supersaturated solution.

To give further evidence for the conclusion we have achieved above, fluorescence spectra and TEM images of 1.0 mg/mL $C_{60}$-pyridine solution after centrifugal separation are displayed in Figure 4. As we can see in Figure 4a, the fluorescence of the $C_{60}$-pyridine solution consists of three strong fluorescence bands centered at 440, 575, and 700 nm, respectively. After centrifugal separation at 1200 revolutions/s for 5 min, the solution is separated into two layers (i.e., the upper purple settled solution

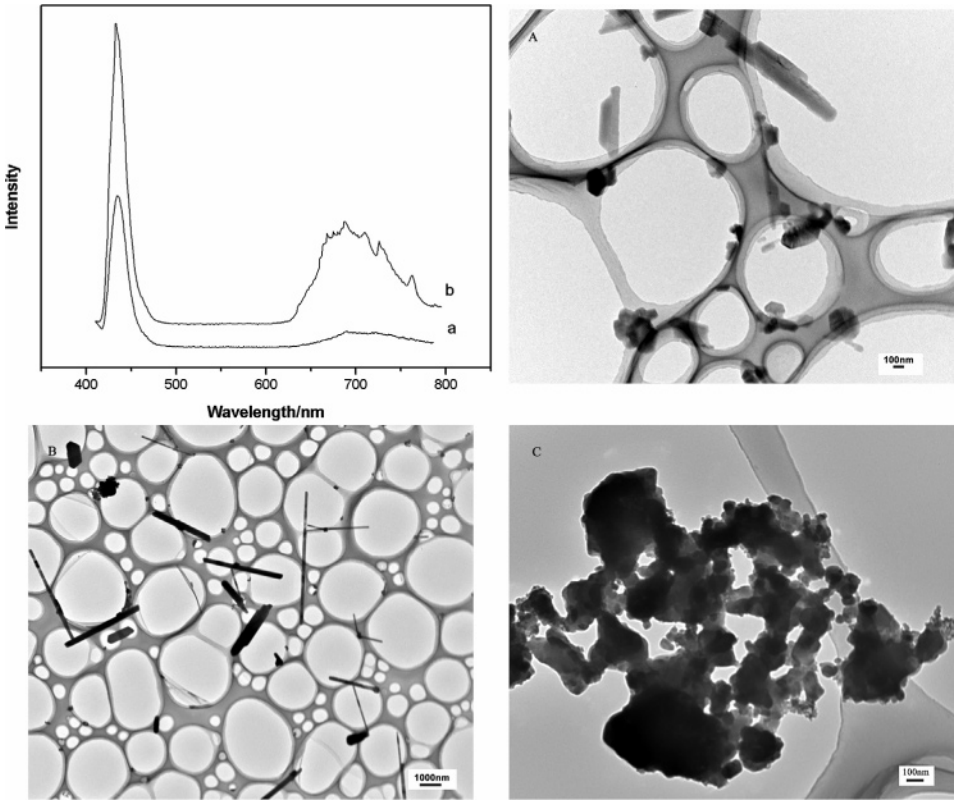


**Figure 5.** Fluorescence spectra of $C_{60}$-toluene solutions settled for (a) 7 h and (b) 7 min. In-situ TEM images corresponding to (A) spectrum a, (B and C) spectrum b.

and the lower brownish-black opaque solution). From the up layer solution, a fluorescence band at 440 nm appears apparently (Figure 4b) in company with the in-situ TEM image (Figure 4B) exhibiting the only presence of $C_{60}$ nanoparticals. So far, it can be approved that the fluorescence band located at 440 nm originates from $C_{60}$ nanoparticals.

Comparatively, no fluorescence peaks in the UV portion emitted from the low layer brownish-black solution, and only two fluorescence bands centered at 575 and 700 nm were achieved as shown in Figure 4c. After several processes of diluting and centrifugal separating, the color of this solution turns to brownish-yellow. Only the band at 575 nm is present with a strong relative intensity (Figure 4d) with the in-situ TEM image (Figure 4D) exhibiting that $C_{60}$ in this solution is almost in the existence of lace-like cluster, as provides an eloquent evidence to the conclusion that the fluorescence band centered at 575 nm arises from $C_{60}$ lace-like cluster.

Additionally, as for the color change of solution from dark to light after dilution and centrifugation, it is considered as the result of a gradual dissolving of $C_{60}$ microbulks into the solution. The simultaneous decay of a band centered at 700 nm in Figure 4d is very compatible with the conclusion that the fluorescence band centered at 700 nm is emitted from bulk $C_{60}$ in supersaturated solution.

To gain more confidence in our assignments for the three strong fluorescence bands of $C_{60}$ in pyridine, fluorescence measurements and TEM observations were taken on the $C_{60}$-toluene system as well. Figure 5a shows the fluorescence spectrum of 3.0 mg/mL $C_{60}$-toluene solution that is settled for 7 h. As we can see, with most of $C_{60}$ dissolved in solution being in the existence of particles with an average diameter of 80 nm (Figure 5a), two fluorescence bands located at 440 and 700 nm are observed. Especially, the blue fluorescence band is of about 6 times stronger in intensity than the structureless salmon pink fluorescence band. Correspondingly, when the settle time for the 3.0 mg/mL $C_{60}$-toluene solution was reduced to 7 min, it can be seen that, with the emergence of plenty of solvate crystalline $C_{60}$ (Figure 5b) and unsolvated $C_{60}$ microblocks (Figure 5c), the fluorescence band located at 700 nm (Figure 5b) is enhanced by a factor of 2 in relative intensity. From the evidence presented above, the previous attributions of fluorescence bands centered at 440 and 700 nm in supersaturate $C_{60}$-pyridine solution can be further confirmed.

As for the distinctive fine structures of $C_{60}$ fluorescence band around 440 nm in toluene and pyridine, we believe it is a result of the characteristic interaction between $C_{60}$ and solvents. While the general identity of the $C_{60}$ fluorescence bands centered at 700 nm in the two solvents may account for the weak solvent effect on $C_{60}$ in the solid matrix. In addition, it is also noticed that the fluorescence band at 575 nm disappears with the absence of lace-like clusters of $C_{60}$ in the $C_{60}$-toluene system, which not only agrees well with the fact that the formation of lace-like clusters of $C_{60}$ is related to the special interaction between $C_{60}$ and pyridine but also is compatible with the conclusion that yellow-green fluorescence band centered at 575 nm originates from $C_{60}$ lace-like cluster.

## Conclusion

In collusion, the nanostructure origins of the three strong fluorescence emission bands of $C_{60}$ in room-temperature pyridine are reported for the first time. Through fluorescence and TEM observation carried out on the $C_{60}$-pyridine solution settled for different times, it is revealed that the blue fluorescence peaks centered at 440 nm derives from $C_{60}$ nanoparticles; the yellow-green fluorescence band located at 575 nm arises from $C_{60}$ lace-like cluster; the salmon pink fluorescence band around 700 nm originates from microbulk $C_{60}$ in solution. And the conclusions above are supported by further investigations on the $C_{60}$-toluene

system as well. In a word, solvent-induced nanostructure determines the interaction pattern of $C_{60}$ with solvent, and thus the shape and color of $C_{60}$ fluorescence band in solution may not only open a doorway for further systematic studies of fluorescence of $C_{60}$ in solution but also provide a novel application potential of fullerne in white light photosensitive and luminescent material.

**Acknowledgment.** The authors are grateful for the support of this research by the National Natural Science Foundation of China and the Natural Science Foundation of Beijing.

## References and Notes

(1) Schick, G.; Levitus, M.; Kvetko, L. D.; Johnson, B. A.; Lamparth, I.; Lunkwitz, R.; Ma, B.; Khan, S. I.; Garcia-Garibay, M. A.; Rubin, Y. *J. Am. Chem. Soc.* **1999**, *121*, 3246−3247.

(2) Gupta N.; Santhanam, K. S. V. *Chem. Phys.* **1994**, *185*, 113.

(3) Cheng, J.-x.; Fang, Y.; Huang, Q.-j.; Yan, Y.-J.; Li, X.-Y. *Chem. Phys. Lett.* **2000**, *330*, 262.

(4) Krätschmer, W.; Lamb, L. D.; Fostiropoulos, K.; Huffman, D. R. *Nature* **1991**, *347*, 354.

(5) Bethune, D. S.; Meijer, G.; Tang, W. C.; Rosen, H. J. *Chem. Phys. Lett.* **1990**, *174*, 219.

(6) Johnson, R. D.; Meijer, G.; Bethune, D. S. *J. Am. Chem. Soc.* **1990**, *112*, 8983.

(7) van den Heuvel, D. J.; van den Berg, G. J. B.; Groenen, E. J. J.; Schmidt, J. *J. Phys. Chem.* **1995**, *99*, 11644.

(8) Wang, Y. *J. Phys. Chem.* **1992**, *96*, 764.

(9) Zeng, Y.; Biczok, l.; Linschitz, H. *J. Phys. Chem.* **1992**, *96*, 5237.

(10) Reber, C.; Yee, L.; McKiernan, J. I.; Williams, R. S.; Tong, W. M.; Ohlberg, D. A. A.; Whetten, R. L.; Diederich, F. *J. Phys. Chem.* **1991**, *95*, 187.

(11) Sauvajol, J. L.; Hricha, Z.; Coustel, N.; Zahab, A. *Aznar J. Phys.: Condens. Matter* **1993**, *5*, 2045.

(12) Sibley, S. P.; Argentine, S. M.; Francis, A. H. *Chem. Phys. Lett.* **1992**, *188*, 187.

(13) Xia, A.; Pan, H.; Zhang, X.; Hong, Y.; Fu, S.; Shi, J.; Zuo, J.; Xu, C. *J. Lumin.* **1995**, *63*, 301.

(14) Kim, D.; Lee, M. *J. Am. Chem. Soc.* **1992**, *114*, 4429.

(15) Zhao, Y.; Fang, Y. *J. Phys. Chem.* **2004**, *108*, 13586.

(16) Herzberg, E.; Teller, Z. *Phys. Chem. B* **1933**, *21*, 410.

(17) Korobov, M. V.; Mirakyan, A. L.; Avramenko, N. V.; Stukalin, E. B. *J. Phys. Chem. B* **2002**, *105*, 2499.

(18) Feldmann, J.; Guss, W.; Lemmer, U.; Göebl, E. O.; Taliani, C.; Mohn, H.; Müller, W.; Häussler, P.; Ter Meer, H.-U. *Mol. Cryst. Liq. Cryst.* **1994**, *256*, 757.

(19) Hutchison, K.; Sichick, J. G.; Rubin, Y.; Wudl, F. *J. Am. Chem. Soc.* **1999**, *121*, 5611.

(20) Kaneto, K.; Abe, T.; Takashima, W. *Solid State Commun.* **1995**, *96*, 259.

(21) Yang, X.-C.; Fang, Y. *J. Phys. Chem. B* **2003**, *107*, 10100.

(22) Reber, C.; Yee, L.; McKiernan, J.; Zink, J. I.; Williams, R. S.; Tong, W. M.; Ohlberg, D. A. A.; Whetten, R. L.; Diederich, F. *J. Phys. Lett.* **1991**, *95*, 2127.

(23) Arbogast, J. W.; Darmanyan, A. P.; Foote, C. S.; Rubin, Y.; Diederich, F. N.; Alvarez, M. M.; Anz, S. J.; Whetten, R. L. *J. Phys. Chem.* **1991**, *95*, 11.